

# Nanocrystalline and non-crystalline hydrides synthesized by controlled reactive mechanical alloying/milling of Mg and Mg–X (X = Fe, Co, Mn, B) systems

R.A. Varin<sup>a,\*</sup>, S. Li<sup>a,b</sup>, Ch. Chiu<sup>a</sup>, L. Guo<sup>a</sup>, O. Morozova<sup>c</sup>,  
T. Khomenko<sup>c</sup>, Z. Wronski<sup>d</sup>

<sup>a</sup> Department of Mechanical Engineering, University of Waterloo, Waterloo, Ont., Canada N2L 3G1

<sup>b</sup> State Key Laboratory for Powder Metallurgy, Central South University, Changsha 410083, PR China

<sup>c</sup> Semenov Institute of Chemical Physics, Russian Academy of Sciences, 119991 Moscow, Russia

<sup>d</sup> CANMET's Material Technology Laboratories, Natural Resources Canada, 568 Booth St., Ottawa, Ont., Canada K1A 0G1

Received 2 June 2004; received in revised form 26 November 2004; accepted 7 December 2004

Available online 14 July 2005

## Abstract

The results of the mechano-chemical synthesis of hydrides by controlled reactive mechanical alloying/milling (CRMA/CRMM) of Mg, 2Mg–Fe, 2Mg–Co, 3Mg–Co, 3Mg–Mn and Mg–2B systems under hydrogen in the magneto-mill Uni-Ball-Mill 5, are discussed. Mostly *nanocrystalline* hydrides have been synthesized in all the above systems while *non-crystalline* (possibly *amorphous*) hydrides have also been synthesized in the 2Mg–Fe system. Double DSC hydrogen desorption peak is observed for a single-phase  $\beta$ -MgH<sub>2</sub> hydride and a single desorption peak is observed for a duplex hydride ( $\beta$ -MgH<sub>2</sub> + Mg<sub>2</sub>FeH<sub>6</sub>). The effects of initial nanograin (crystallite) size (after synthesis by CRMA) and alloy composition on the DSC hydrogen desorption temperature of  $\beta$ -MgH<sub>2</sub> and Mg<sub>2</sub>FeH<sub>6</sub> are presented.

© 2005 Elsevier B.V. All rights reserved.

**Keywords:** Hydrogen storage materials; Reactive mechanical alloying/milling; Non-crystalline hydrides; X-ray diffraction; Thermal analysis; Calorimetry and temperature programmed desorption

## 1. Introduction

The key roadblock to the widespread use of hydrogen as a renewable fuel on-board of passenger vehicles is hydrogen storage [1] and the highest potential has the solid hydrogen storage in complex hydrides [2]. In the first phase of our on-going research program on *nanostructured* materials for hydrogen storage we have focused on the complex hydrides based on abundant and inexpensive Mg metal. In the systems 2Mg–Fe, 2Mg–Co, 3Mg–Mn, Mg–2Al and Mg–2B the complex hydrides such as Mg<sub>2</sub>FeH<sub>6</sub> [3], Mg<sub>2</sub>CoH<sub>5</sub> [4], Mg<sub>3</sub>MnH<sub>7</sub> [5], Mg(AlH<sub>4</sub>)<sub>2</sub> [6,7] and Mg(BH<sub>4</sub>)<sub>2</sub> [8], respectively, have been already synthesized by mostly wet

chemical methods or by sintering at high temperatures under high hydrogen pressure. The principal synthesis method in our on-going program is the mechano-chemical synthesis in a solid state by controlled reactive mechanical alloying/milling (CRMA/CRMM) under hydrogen in the magneto-mill Uni-Ball-Mill 5 (A.O.C. Scientific Engineering Pty Ltd., Australia). CRMA is a one-step method in which the hydride synthesis accompanied by *nanostructuring* of phases occurs in due course of milling facilitating in-situ formation of nanocrystalline (nanostructured) hydrides [9]. There are a couple of clear advantages of CRMA/CRMM: (a) the required initial activation and hydrogenation after conventional mechanical alloying/milling (MA/MM) in a two-step synthesis can be avoided reducing the cost, and (b) it is possible to “composite” Mg-based complex hydrides with higher gravimetric density but much more expensive

\* Corresponding author. Fax: +1 519 888 6197.

E-mail address: ravarin@mecheng1.uwaterloo.ca (R.A. Varin).

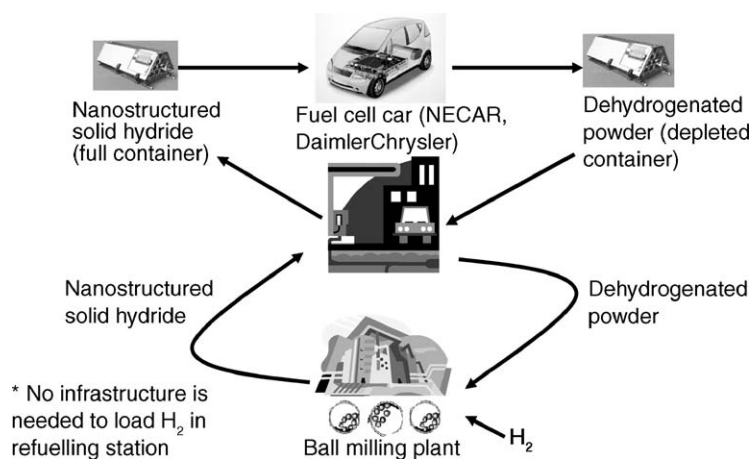


Fig. 1. A future vision of commercial manufacturing of hydrides for solid state hydrogen storage by reactive mechanical alloying under hydrogen and their cycling which in effect will eliminate costly hydrogen infrastructure from the refuelling stations for fuel cell powered automobiles.

complex hydrides such as, for example,  $\text{LiBH}_4$  [10], to produce less expensive *nanocomposite complex hydrides* with possibly reduced desorption temperature and more rapid desorption kinetics. Furthermore, our vision for the future is that the widespread commercialization of reactive mechanical alloying/milling under hydrogen to manufacture hydrides could essentially eliminate the requirement of costly hydrogen infrastructure at the refuelling stations for fuel cell powered automobiles as schematically shown in Fig. 1.

In this paper we will present results, some of them rather puzzling, which we have recently obtained during CRMA/CRMM attempts to synthesize the Mg-based binary and complex hydrides. Formation of *non-crystalline* (possibly amorphous) hydrides in the 2Mg–Fe system and their thermal hydrogen desorption will also be presented. Some puzzling phenomena such as DSC peak doublets will be presented and discussed. The effect of nanograin (crystallite) size and alloy composition on the hydrogen desorption temperature of  $\beta\text{-MgH}_2$  and  $\text{Mg}_2\text{FeH}_6$  will also be critically assessed.

## 2. Experimental

Elemental powders of pure Mg and pure Fe, Co, Mn and B were mixed in the appropriate stoichiometric compositions and subjected to controlled reactive mechanical alloying/milling (CRMA/CRMM) in the magneto-mill, Uni-Ball-Mill 5 (A.O.C. Scientific Engineering Pty Ltd., Australia), under elemental milling modes such as *shearing* and *impact*. More extensive details of milling procedures can be found in a number of Refs. [11–15]. Morphological and microstructural examination of powders was conducted using high-resolution, field emission SEM (FE SEM) LEO 1530 equipped with integrated EDAX Pegasus 1200 EDS/OIM and X-ray diffraction [11–15]. Thermal behavior was investigated by DSC, TGA [13–15] and temperature programmed desorption (TPD) [14,15].

## 3. Results and discussion

Fig. 2a shows the XRD pattern of the 2Mg–Fe mixture subjected to CRMA under hydrogen for 59 h under *low-energy shearing* mode [13]. Only the peaks of retained unreacted Fe are observed while no peaks of crystalline hydrides are detected although after shorter milling time of this powder the  $\beta\text{-MgH}_2$  hydride was indeed present [13]. Four samples of powders reactively milled for 59 h under *shearing* clearly desorbed hydrogen in DSC test as evidenced in Fig. 2b by deep endothermic peaks, within the temperature range of  $\sim 321\text{--}329^\circ\text{C}$ . The  $\text{H}_2$  amount from TGA test was estimated at  $\sim 2.5$  wt.%. Additional TPD test [14] confirmed the desorption of  $\sim 3.8$  wt.% hydrogen at  $\sim 306^\circ\text{C}$  (Fig. 2c). Another example of a similar behavior for a powder mixture processed under *low-energy impact* (IMP1) mode is shown in Fig. 3. The XRD pattern in Fig. 3a of the mixture 2Mg–Fe subjected to CRMA for 210 h shows the presence of retained unreacted Fe and a small amount of MgO but no crystalline hydrides are present. Fig. 3b shows a single DSC endothermic hydrogen desorption peak. The  $\text{H}_2$  amount from TGA test was estimated at  $\sim 2.0$  wt.%. Since no crystalline hydrides are detected by XRD (Figs. 2 and 3), it must be concluded that in both cases the hydrogen must have been released from *non-crystalline* (amorphous) hydrides. However, the exact nature of these hydrides still remains elusive.

Fig. 4a shows the XRD pattern of a mixture of nanostructured duplex hydride ( $\text{Mg}_2\text{FeH}_6 + \beta\text{-MgH}_2$ ) synthesized after CRMA for 100 h under *high-energy impact* (IMP2) mode [15]. However, despite the presence of two dissimilar hydrides, the DSC curve shows only a perfectly symmetrical single endothermic peak with the maximum at  $\sim 275^\circ\text{C}$  (Fig. 4b). TGA gave  $\sim 2.4$  wt.% of desorbed hydrogen [15]. It is not clear why only a single DSC peak is observed for hydrogen desorption from a mixture of two dissimilar hydride species.

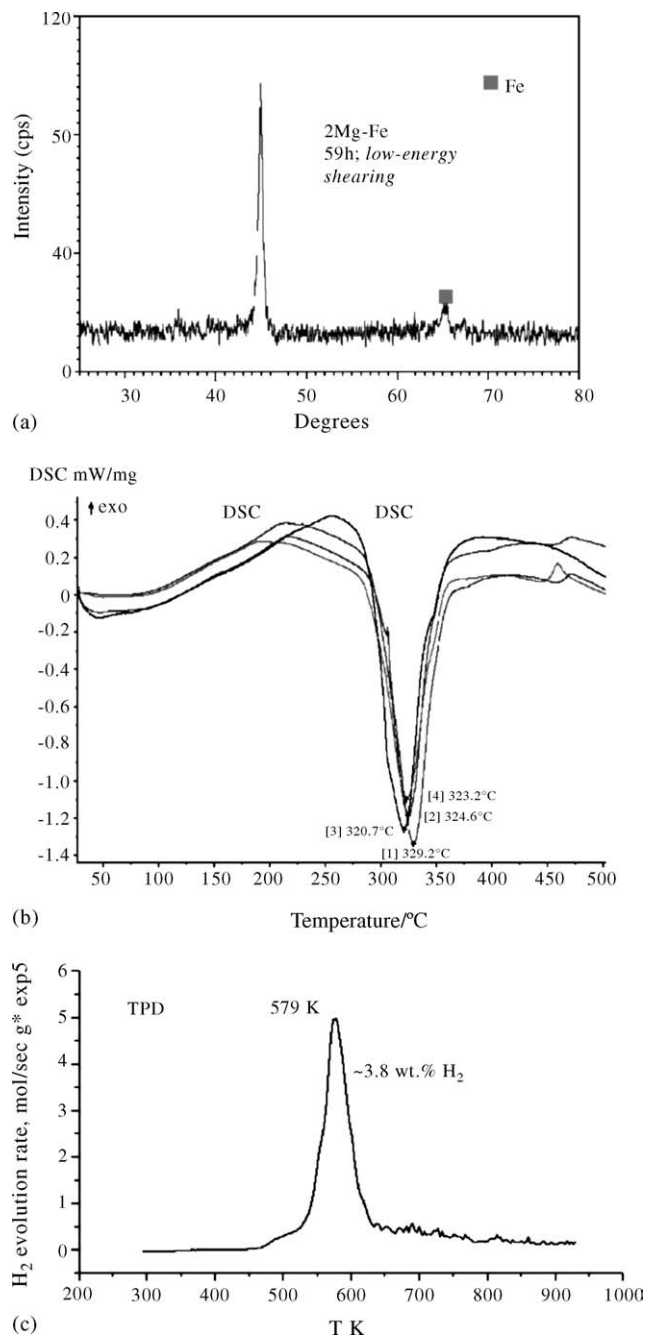


Fig. 2. Behavior of the 2Mg–Fe mixture subjected to CRMA under hydrogen for 59 h under low-energy shearing mode. (a) XRD pattern without any peaks of crystalline hydrides, (b) DSC desorption of hydrogen for four powder samples and (c) TPD desorption peak of  $\sim 3.8$  wt.%  $H_2$  at  $\sim 306^\circ C$ . Adopted from [13].

Fig. 5a shows DSC curve of a single-phase  $\beta$ -MgH<sub>2</sub> hydride synthesized by CRMM under *high-energy shearing* mode of pure Mg under hydrogen for 150 h. A double endothermic peak of desorption, split into individual peaks at 354 and 382 °C, is observed. To analyze the origin of a double peak two DSC runs were stopped at 373 and 500 °C, i.e. above the lower- and higher-temperature peak at 354 and 382 °C, respectively. Fig. 5b shows the XRD pattern of

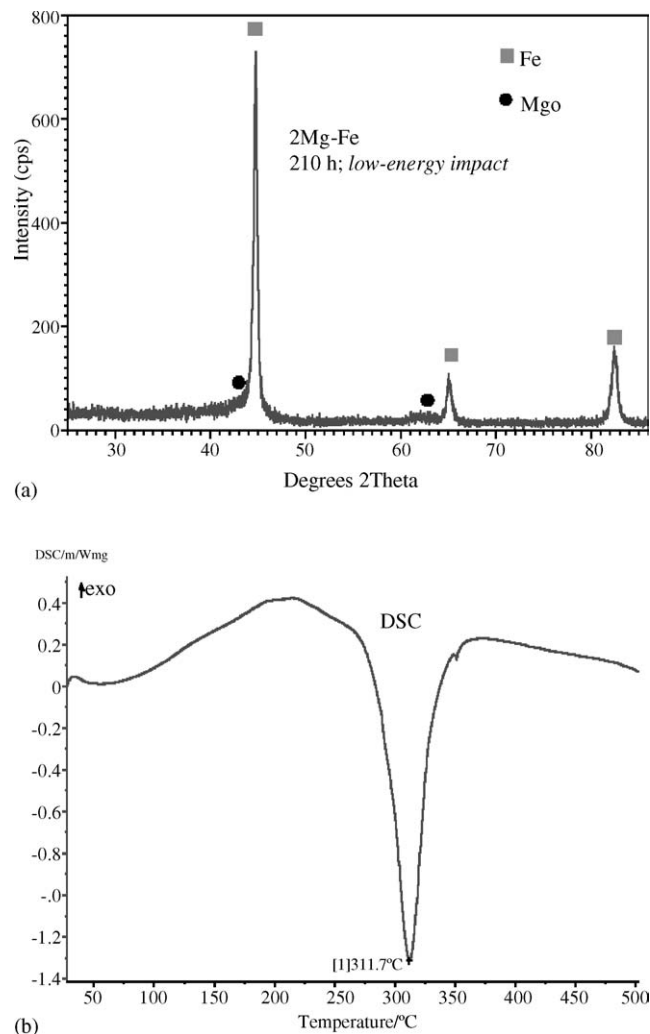


Fig. 3. (a) XRD pattern of 2Mg–Fe mixture subjected to CRMA under hydrogen for 210 h under low-energy impact mode. (b) DSC curve with an endothermic peak of hydrogen desorption. Adopted from [14].

as-milled powder with clear peaks of  $\beta$ -MgH<sub>2</sub> and the XRD patterns of heated powders. Some remnant  $\beta$ -MgH<sub>2</sub> is still present after heating to 373 °C but it completely decomposes at 500 °C. Apparently, a single-phase  $\beta$ -MgH<sub>2</sub> decomposed by a peculiar two-step mechanism which is reported here for the first time. At the moment only a speculative mechanism can be put forward to account for the observed peak doublet. The large intensity of the MgO XRD peaks in Fig. 5b indicates that some oxidation have occurred to form an MgO barrier on portions of the  $\beta$ -MgH<sub>2</sub> particles (i.e. perhaps smaller size ones). The oxidation might have inhibited hydrogen release from this fraction of particles during DSC test until either cracking or permeation of the surface oxides had occurred at higher temperature of desorption. However, whether or not the oxidation of MgH<sub>2</sub> to form MgO is a feasible mechanism remains to be seen.

Fig. 6a shows the DSC hydrogen desorption peak temperatures plotted as a function of the initial nanograin (crystallite) size of binary MgH<sub>2</sub> after synthesis by CRMA

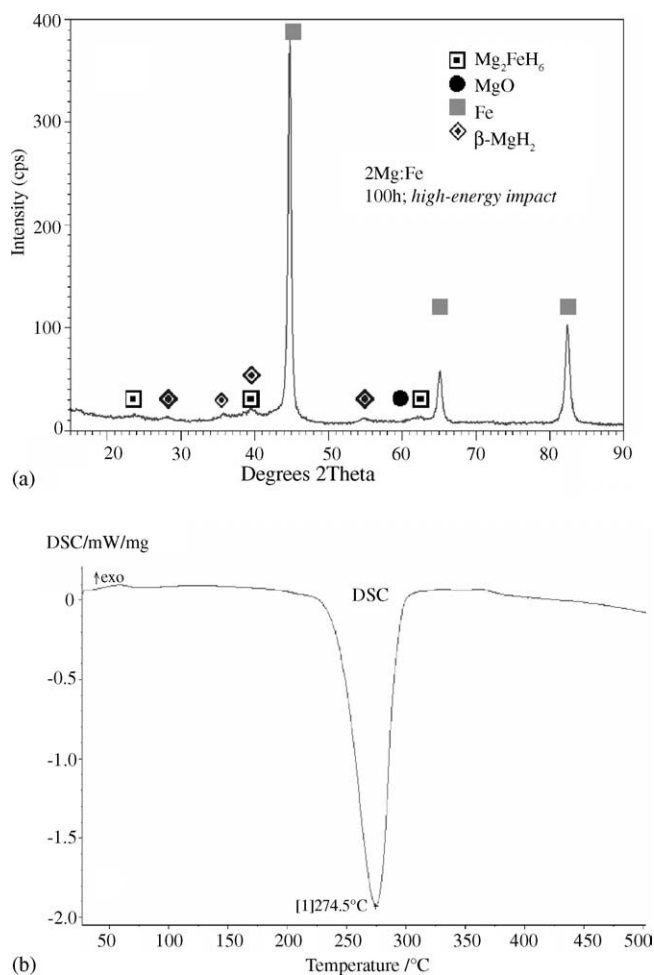


Fig. 4. (a) XRD pattern of 2Mg–Fe elemental mixture subjected to 100 h of CRMA under hydrogen under high-energy impact mode. (b) DSC curve of the same mixture. Adopted from [15].

in various powder mixtures. The DSC desorption peak temperature of  $\beta$ -MgH<sub>2</sub> and the mixture of ( $\beta$ -MgH<sub>2</sub> +  $\gamma$ -MgH<sub>2</sub>) found in the 2Mg–Fe, 2Mg–Co, 3Mg–Co, 3Mg–Mn and Mg–2B systems after CRMA shows no systematic dependence on nanograin (crystallite) size of  $\beta$ -MgH<sub>2</sub> within the investigated size range 2–21 nm (Fig. 6a). However, the upper bound and lower bound of DSC peak temperatures is limited by Mg–2B and 2Mg–Fe systems, respectively, indicating a strong alloying element effect (Fig. 6a). It must be clarified that in the 2Mg–Co, 3Mg–Co and 3Mg–Mn mixtures subjected to CRMA under *low-energy shearing* mode only equilibrium  $\beta$ -MgH<sub>2</sub> has been synthesized [16,17] whereas under *high-energy shearing* and *low-energy impact* modes two allotropic forms of MgH<sub>2</sub>: equilibrium  $\beta$ -MgH<sub>2</sub> and metastable  $\gamma$ -MgH<sub>2</sub> [18,19] (designated b-MgH<sub>2</sub> and g-MgH<sub>2</sub> in the legend to Fig. 6, respectively), have been synthesized [17]. However, no ternary complex hydrides Mg<sub>2</sub>CoH<sub>5</sub> and Mg<sub>3</sub>MnH<sub>7</sub> have been formed [16,17]. The DSC curves of the milled powders containing ( $\beta$ -MgH<sub>2</sub> +  $\gamma$ -MgH<sub>2</sub>) showed an endothermic double peak (doublet) in which a lower temperature peak is attributed to the total decomposition of

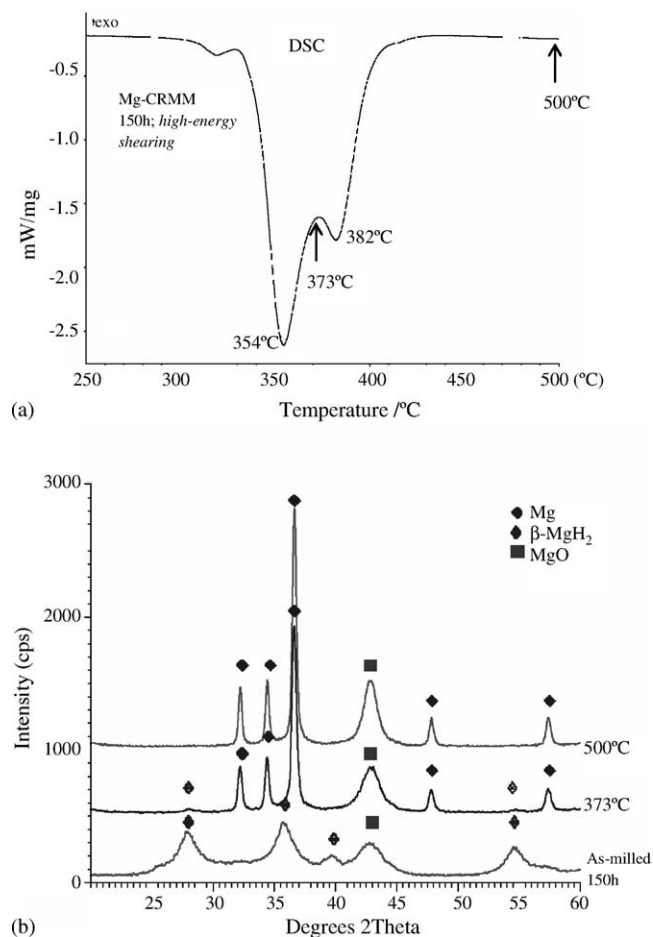


Fig. 5. (a) DSC curve of Mg–H powder after controlled reactive mechanical milling (CRMM) for 150 h under high-energy shearing mode. (b) XRD patterns of Mg–H powder after CRMM for 150 h and after stopping DSC run at 373 and 500 °C.

$\gamma$ -MgH<sub>2</sub> and partial of  $\beta$ -MgH<sub>2</sub> whereas a higher temperature peak is attributed to the desorption from the remnant  $\beta$ -MgH<sub>2</sub> [17].

Similarly to the behavior of MgH<sub>2</sub>, the DSC hydrogen desorption peak temperature of the nanostructured ternary complex hydride Mg<sub>2</sub>FeH<sub>6</sub> and the duplex mixture ( $\beta$ -MgH<sub>2</sub> + Mg<sub>2</sub>FeH<sub>6</sub>), synthesized in a number of differently milled Mg–Fe and 2Mg–Fe mixtures [14,15], does not seem to depend on the initial nanograin (crystallite) size of Mg<sub>2</sub>FeH<sub>6</sub> (within the investigated range 2–8 nm) (Fig. 6b). In addition, no correlation of desorption temperature with Mg<sub>2</sub>FeH<sub>6</sub> existing as either a single-phase hydride or a duplex ( $\beta$ -MgH<sub>2</sub> + Mg<sub>2</sub>FeH<sub>6</sub>) hydride is observed in Fig. 6b. Interestingly, most of the recorded desorption temperatures for this nanostructured system are much lower than 300 °C although a few data points are over 300 °C (Fig. 6b). A substantial difference between the desorption temperatures of differently milled powders in Fig. 6b seems to demonstrate that there may be other factors strongly affecting the DSC hydrogen desorption temperature than just the initial crystallite size of Mg<sub>2</sub>FeH<sub>6</sub> hydride. Possibly, one of those factors



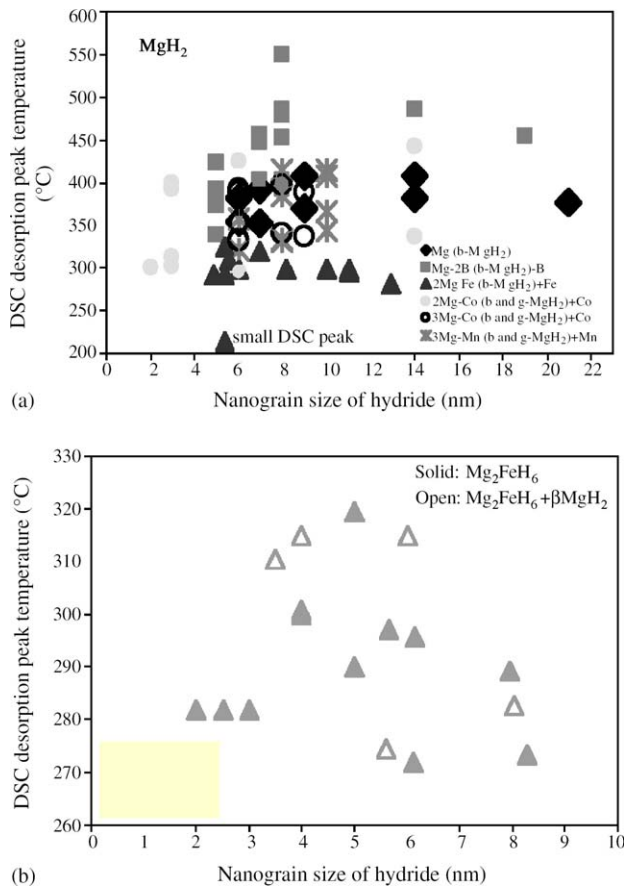


Fig. 6. Dependence of DSC desorption peak temperature of (a)  $\text{MgH}_2$  on the initial nanograin (crystallite) size of  $\beta\text{-MgH}_2$ , and (b)  $\text{Mg}_2\text{FeH}_6$  and duplex mixture of ( $\beta\text{-MgH}_2 + \text{Mg}_2\text{FeH}_6$ ) on the initial nanograin (crystallite) size of  $\text{Mg}_2\text{FeH}_6$ . In the legend “b” is  $\beta$  and “g” is  $\gamma$ .

might be a powder particle size distribution after milling. This problem needs further studies.

#### 4. Conclusions

*Non-crystalline* (possibly *amorphous*) hydrides are observed after CRMA of  $2\text{Mg-Fe}$  elemental mixture under *low-energy shearing* and *low-energy impact* mode. They desorb hydrogen in the amount of  $\sim 2.0$  to  $3.8$  wt.%. However, their nature still remains elusive. A DSC curve of a single-phase  $\beta\text{-MgH}_2$  synthesized by CRMM for 150 h under *high-energy shearing* mode shows a double endothermic peak on hydrogen desorption. A DSC curve of the  $2\text{Mg-Fe}$  milled powder containing a duplex mixture of ( $\beta\text{-MgH}_2 + \text{Mg}_2\text{FeH}_6$ ) shows only a single and perfectly symmetrical endothermic

peak for hydrogen desorption. The highest and lowest DSC desorption peak temperature bound for  $\text{MgH}_2$  desorption is observed for the  $\text{Mg-2B}$  and  $2\text{Mg-Fe}$  system, respectively, which demonstrates a strong effect of alloying element. There is no systematic dependence of DSC hydrogen desorption peak temperature on the initial nanograin (crystallite) size of both  $\beta\text{-MgH}_2$  and  $\text{Mg}_2\text{FeH}_6$  hydrides.

#### Acknowledgements

This work was supported by a grant from the Natural Sciences and Engineering Research Council of Canada, which is gratefully acknowledged.

#### References

- [1] J.A. Ritter, A.D. Ebner, J. Wang, R. Zidan, *Mater. Today* (2003) 18–23.
- [2] B. Bogdanovi, G. Sandrock, *MRS Bull.* 27 (2002) 712–716.
- [3] J.-J. Didisheim, P. Zolliker, K. Yvon, P. Fischer, J. Schefer, M. Gubelmann, A.F. Williams, *Inorg. Chem.* 23 (1984) 1953–1957.
- [4] P. Zolliker, K. Yvon, P. Fischer, J. Schefer, *Inorg. Chem.* 23 (1985) 4177–4187.
- [5] M. Bortz, B. Bertheville, K. Yvon, E.A. Movlaev, V.N. Verbetsky, F. Fauth, *J. Alloys Compd.* 279 (1998) L8–L10.
- [6] E.C. Ashby, R.D. Schwartz, B.D. James, *Inorg. Chem.* 9 (1970) 325–332.
- [7] M. Fichtner, O. Fuhr, *J. Alloys Compd.* 345 (2002) 286–296.
- [8] V.N. Konoplev, V.M. Bakulina, *Izv. Akad. Nauk SSSR; Ser. Khimicheskaya* (1) (1971) 159–161.
- [9] J.-L. Bobet, B. Chevalier, M.Y. Song, B. Darriet, J. Etourneau, *J. Alloys Compd.* 336 (2002) 292–296.
- [10] A. Züttel, P. Wenger, S. Rentsch, P. Sudan, Ph. Mauron, Ch. Emmenegger, *J. Power Source* 118 (2003) 1–7.
- [11] R.A. Varin, T. Czujko, J. Mizera, *J. Alloys Compd.* 350 (2003) 332–339.
- [12] R.A. Varin, T. Czujko, J. Mizera, *J. Alloys Compd.* 354 (2003) 281–295.
- [13] R.A. Varin, S. Li, A. Calka, D. Wexler, *J. Alloys Compd.* 373 (2004) 270–286.
- [14] S. Li, R.A. Varin, O. Morozova, T. Khomenko, *J. Alloys Compd.* 384 (2004) 231–248.
- [15] R.A. Varin, S. Li, Z. Wronski, O. Morozova, T. Khomenko, *J. Alloys Compd.* 390 (2005) 282–296.
- [16] L. Guo, M.A.Sc. Thesis, University of Waterloo, May 2004.
- [17] R.A. Varin, L. Guo, in: T.S. Srivatsan, R.A. Varin (Eds.), *Proceedings of the International Symposium on Processing and Fabrication of Advanced Materials XII-PFAM XII*, ASM International, Materials Park, OH (2004), pp. 407–429.
- [18] R. Schulz, J. Huot, G. Liang, S. Boily, A. Van Neste, *Mater. Sci. Forum.* 312–314 (1999) 615–622.
- [19] R. Schulz, J. Huot, G. Liang, S. Boily, G. Lalande, M.C. Denis, J.P. Dodelet, *Mater. Sci. Eng. A* 267 (1999) 240–245.